# We are IntechOpen,
# the world's leading publisher of
# Open Access books
# Built by scientists, for scientists

## 6,900
Open access books available

## 186,000
International authors and editors

## 200M
Downloads

Our authors are among the

## 154
Countries delivered to

## TOP 1%
most cited scientists

## 12.2%
Contributors from top 500 universities

CLARIVATE ANALYTICS

**BOOK CITATION INDEX**

INDEXED

**WEB OF SCIENCE**™

Selection of our books indexed in the Book Citation Index
in Web of Science™ Core Collection (BKCI)

# Interested in publishing with us?
# Contact book.department@intechopen.com

Numbers displayed above are based on latest data collected.
For more information visit www.intechopen.com

# Integral Equation Analysis with Characteristic Basis Functions

Jaime Laviada, Fernando Las-Heras and
Marcos R. Pino

Additional information is available at the end of the chapter

http://dx.doi.org/10.5772/50502

## 1. Introduction

Full-wave electromagnetic analysis algorithms dependence on the number of unknowns $N$. The complexities ranges from $O(N \log N)$ for certain iterative schemes such as the fast multipole method [8,42] or the adaptive integral method [5] to $O(N^3)$ for the conventional method of moments (MoM) [20].

Thus, the reduction of the number of unknowns results very attractive since it reduces the demanded computational resources in terms of memory and CPU time. In the method of moments context, the choice of the basis functions has a strong impact on the degrees of freedom that are required to solve the problem and, therefore, strategies for unknowns reduction are based on choosing the basis functions as good as possible.

Conventional piecewise basis functions such as Rao-Wilto-Glisson (RWG) [40] or rooftops [15], involve an expansion that is able to model almost any kind of current. Thus, it could be convenient to limit the set of basis functions so that is is only made of that ones which can model currents with a physical meaning and, therefore, to reduce the number of degrees of freedom of the problem under analysis. It is well-known that entire-domain basis functions enable a very efficiently modeling of the currents. Nonetheless, the computation of a set of entire-domain basis functions it is only possible for certain canonical geometries [44,31,4] or via numerical techniques which involve solving the entire problem [19,18] with the corresponding computational cost.

The basis functions to be used for solving our problem should be able to model any kind of current that could be induced in the geometry under analysis. In a general analysis, it is not possible to obtain a finite and complete set of basis functions unless the conditions of the

problem are strongly restricted. Nonetheless, it will be shown in this book chapter that it is possible to compute a set of basis functions that can be progressively increased to reach an accuracy similar to the accuracy that would be achieved by means of low-level basis functions (RWG, rooftops, etc.).

The entire-domain basis functions are usually expressed as linear combinations of low-level basis functions. This definition enables an easy and efficient computation of the system of equations matrix since it is possible to exploit the linear properties of the integral equations to carry out the computation.

Among the pioneering works on this field, we find the theory of *characteristic modes* that has been carry out by Harrington [19,18]. This modes are computed by solving the following generalized eigenvalue problem:

$$\overline{\overline{X}} \, \overline{I}_n = \lambda_n \overline{\overline{R}} \, \overline{I}_n \qquad (1)$$

where the matrices $\overline{\overline{R}}$ and $\overline{\overline{X}}$ are the real and imaginary part of the impedance matrix, respectively. The impedance matrix should have been computed from the EFIE with the Galerkin's method. Thus, the eigenvalues, $\lambda_n$, and eigenvectors, $I_n$, will be real due to the symmetries. The choice of the eigenvectors as basis functions yields a diagonal matrix with the corresponding computational advantages. If the geometry under analysis is modeled with $N$ conventional low-level basis functions (e.g., RWG or rooftop), the number of eigenvalues will be also $N$. This eigenvalues are a complete base that can model any current with the same accuracy as the one that could be achieved with the $N$ low-level basis functions. Nonetheless, the eigenvector with highest eigenvalues will have a more significant contribution to the radiation so that the eigenvectors under a certain threshold can be discarded as basis functions. Thus, it is possible to find a set of basis functions with very good accuracy whose size is smaller than $N$.

During the eighties and nineties, the research on this kind of basis functions was diffused. Nevertheless, the interest on these techniques has reemerged due to the possibilities in the application to the design of antennas [6]. In this research line, the physical meaning of the characteristic modes is exploited for the design of antennas with certain characteristics. The convergence of the accuracy as a function of the number of basis functions is improved by including a source mode that is computed by exciting the antenna and attaching the induced current with the eigenvectors.

Computation of characteristic modes involves the solution of an eigenvalue problem that limits the size of the elements where the basis functions can be defined. For this reason, this technique has been limited to the analysis of arrays with elements that are not connected each other. In addition, once the basis functions has been computed for an element, they can be copied for the rest of the elements and, therefore, to save CPU time. An example of this technique has been shown in [32] where the authors analyze a 3 × 3 antenna array by defining basis functions for each element. In particular, they consider three kinds of elements de-

pending on the position of the element (center, corner or border) and they reuse the same basis function for each kind of element.

A similar problematic happens in the adaptive basis function method that has been proposed in [45]. In this method, a diagonally dominant moment matrix is achieved by building macrobasis functions for a certain body. This macrobasis functions are chosen so that they are orthogonal to the testing functions on the body. This method was also extended in [14,12,13] for the solution of arrays of equally-spaced disconnected elements.

A special case of basis functions defined as aggregation of low-level basis functions is the *Multilevel Method of Moments* [22]. The authors developed an iterative system based on the generation of hierarchical basis functions for the analysis of two-dimensional scattering problems. In this scheme, the solution of the problem was computed by iteratively solving it with basis functions of different sizes so that it enables to refine the solution. Although the aim of these basis functions was not an efficient modeling of the current, it was one of the pioneering on nesting basis functions which will be one of the key point of the techniques presented in this book chapter.

The previous scheme would be modified in [38] for the analysis of printed circuits. In this case, the technique was modified to work with high level basis functions without the need of going back to the low-level basis functions in the intermediate stages. In this method, the circuits were split into blocks and artificial ports were introduced at the end of the blocks. The basis functions were obtained by feeding the natural and the artificial ports and considering the continuity equation for the currents. The extension of this technique for geometries different from printed circuits (e.g. a three-dimensional scatterer) was not accomplished to the authors' best knowledge.

A technique similar to the previous one is the *Subdomain Multilevel Approach* (SMA) [43] for the analysis of certain kind of microstrip circuits. In this method, the geometry is decomposed into several subdomains (e.g. the feeding network and the antennas) and these subdomains are fed by a generator. The induced currents are used as the basis functions which are referred to as macrobasis functions. The rest of the geometry, which is not decomposed into subdomains, is analyzed with conventional basis functions (weak compression) or through new macrobasis functions computed by feeding each port (strong compression). The accuracy of the method is improved by decomposing each macrobasis functions into two basis functions corresponding to the real and imaginary parts. In addition, the joint between macrobasis functions is improved by including rootops between them. The main drawback of this method is also the difficulty to be extended to arbitrary geometries.

The *characteristic basis function method* (CBFM) [39] laid the foundations to generate macrobasis functions for three-dimension arbitrary-shaped scattering and radiation problems. In this first work, the generation of the characteristic basis functions (CBFs) yields two kinds of basis functions primary and secondary ones. This method will be later presented and compared with some new techniques for generating CBFs.

Another method which shares many points in common with the CBFM is the *Synthetic-Functions eXpansion* (SFX) [35]. The different versions of the CBFM [33,11] as well as the SFX can

be considered as a generalization of the Multilevel method of moments and SMA to three-dimensional problems where plane-waves or external dipoles are used instead of artificial ports. This point will be deeply discussed later in section 2.2.

This chapter is structured as follows. Firstly, the theory of the analysis with characteristic basis functions is presented. This first section includes the general basis of any method based on macrobasis functions defined as linear combinations of low-level basis functions, the theoretical consideration of generating CBFs with the external sources method, a comparison of methods for the computation of the reduced matrix and the recursive application of the characteristic basis functions. In the next section, several applications of the CBFM are described including monostatic radar cross section computation, synthesis of phased arrays and analysis of partial modifications on large structures. Finally, the conclusions of the previous sections are summarized.

## 2. Analysis with characteristic basis functions

### 2.1 General basis

The characteristic basis function method pursues to find a set of efficient basis functions so that a smaller number of degrees of freedom is required to solve the problem with the method of moments. The aforementioned basis functions are defined on domains grouping several contiguous low-level basis functions (e.g., RWG or rooftops). In the CBFM context, the domains of definitions of the characteristics basis functions are referred to as *blocks*. Thus, the first step in order to apply the CBFM is to split the geometry under analysis into *B* blocks (see Figure 1).
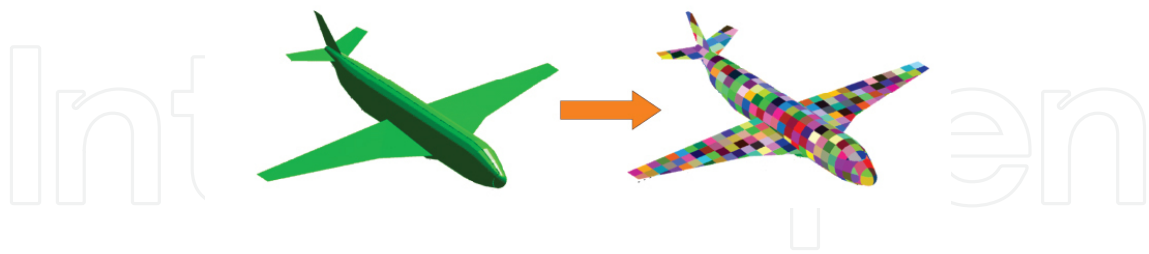


**Figure 1.** Block decomposition for an airplane-like geometry.

On each block, a set of basis functions, which are referred to as characteristic basis functions, are defined. Therefore, the current is expressed as follows:

$$\mathbf{J} = \sum_{i=1}^{B} \sum_{n=1}^{K_i} I_{i,n} \mathcal{F}_{i,n}, \tag{2}$$

where $K_i$ is the number of CBFs in the $i$-th block; $\mathcal{F}_{i,n}$ is the $n$-th CBF in the $i$-th block; and, the coefficients $I_{i,n}$ are the weights of the CBFs in order to express the final solution as a linear combination of the new basis functions. This coefficients are the unknowns to be solved by the method of moments. The CBFs are defined as linear combination of the low-level basis functions:

$$\mathcal{F}_{i,n} = \sum_{m=1}^{N_i} I_{i,m}^{(n)} \mathbf{f}_{i,m} \tag{3}$$

where $N_i$ is the number of low-level basis functions in the $i$-th block; and $f_{i,m}$ is the $m$-th low-level basis functions belonging to the $i$-th block. The definition of the CBFs as a linear combination enables a more simple computation of certain terms such as the reaction terms in the impedance matrix and, therefore, it enables an easy adaptation of previously implemented method of moments codes.

In order to achieve a compact notation, it is useful to define matrices grouping the coefficients of the CBFs for each block. This matrix is defined for the $i$-th block as follows:

$$\bar{\bar{J}}_i = \begin{bmatrix} I_{i,1}^{(1)} & I_{i,1}^{(2)} & \cdots & I_{i,1}^{(K_i)} \\ I_{i,2}^{(1)} & I_{i,2}^{(2)} & \cdots & I_{i,2}^{(K_i)} \\ \vdots & \vdots & \ddots & \vdots \\ I_{i,N_i}^{(1)} & I_{i,N_i}^{(2)} & \cdots & I_{i,N_i}^{(K_i)} \end{bmatrix}. \tag{4}$$

### 2.2 External illumination method

The generation of the CBFs is usually accomplished by means of one of the two following techniques: a) primary and secondary CBFs method; b) external illumination method.

The first method was proposed in the pioneering technique about the CBFM [39] and it was mainly designed for the analysis of arrays of $M$ elements not connected between them. The primary basis functions were obtained by computing the current on each isolated element as a consequence of feeding the port connected to it. Once the primary CBFs are computed for each element, the secondary basis functions for a given element are computed by considering the current induced due to the radiation of the primary CBFs on the rest of the elements. Thus, one primary CBF and $M - 1$ secondary basis functions are defined for each element.

Although the primary and secondary CBFs method has shown an excellent behavior for the analysis of arrays, the accuracy is not so good for scattering problems where the primary CBFs are generated by solving the isolated blocks for the illumination under analysis. In ad-

dition, the CBFs generated by this method depend on the employed incident field and, therefore, they have to be recomputed again if the excitations are changed.

The *external illumination method* was introduced in [33,11] to solve the previous problems. As it will be next shown, the CBFs computed by this technique are a complete set, what has not been proved to be true for the primary and secondary CBFs method.

Let us consider the electric field integral equation for perfect electric conductors (PECs) in terms of the currents induced on each block:

$$0 = \mathbf{E}_i + \sum_{n=1}^{B} \mathcal{L}\left(\mathbf{J}_n\right)\bigg|_t , \tag{5}$$

where $\mathbf{J}_n$ is the current induced in the *n*-th block and $E_i$ is the impressed field. The linear operator $\mathsf{L}(\cdot)$ relates the currents and the electric field radiated by them and it is defined in [7].

If the currents on all the blocks but the *m*-the are known, then the integral equation can be expressed as:

$$-\mathcal{L}\left(\mathbf{J}_m\right)\big|_t = \mathbf{E}_i + \sum_{\substack{n=1 \\ n \neq m}}^{B} \mathcal{L}\left(\mathbf{J}_n\right)\bigg|_t , \tag{6}$$

the solution of (6) yields the current on the block. It is important to observe that if the superposition principle is considered, then the final current on the block can be obtained as a linear combination of the currents induced due to the field radiated by the rest of the blocks and the impressed field.

The field outside a certain block can be expressed as a linear combination of a set of modes which are a complete base for the electromagnetic field. The most common expansions of the field are *spherical-wave expansion* and the *plane-wave expansion*. Another possible expansion is possible by enclosing the block with a surface supporting equivalent magnetic and electric currents which model the radiation due to the sources outside the block. This last expansion is the one used in the SFX [35] where the RWG basis functions are used to model the equivalent currents.

If it is assumed that *any* field impinging the block can be expanded as a discrete and finite set of waves (or as the field radiated by a discretized equivalent current enclosing the block[35]), what can be carried out with arbitrary accuracy by using spherical-or plane-waves (or low-level basis functions), then *any* current induced in the block can be expressed as a linear combination of the currents induced by each wave of the aforementioned set (or by the field radiated by each low-level basis functions).

The approach presented in [33,11] is based on approximating the external illumination by plane-waves. In order to understand this approach, it is important to consider the well-known expressions for plane-wave expansion. These expressions enable us to expand the electric field under a certain plane $z = z_0$ as [17, chapter 3]:

$$\mathbf{E}(\mathbf{r}) = \int_{-\infty}^{\infty}\int_{-\infty}^{\infty} \mathbf{T}(k_x, k_y)e^{-j\mathbf{k}\cdot\mathbf{r}}dk_x dk_y \qquad z \geq z_0, \tag{7}$$

where the vector $\mathbf{T}(k_x, k_y)$ is the *Plane Wave Spectrum* (PWS); and the propagation vector is defined as $k = k_x x + k_y y + k_z z$ with:

$$k_z = \begin{cases} \sqrt{k^2 - k_x^2 - k_y^2}, & k_x^2 + k_y^2 \leq k^2 \\ -j\sqrt{k_x^2 + k_y^2 - k^2}, & k_x^2 + k_y^2 > k^2 \end{cases} \tag{8}$$

It is also possible to use analogous expressions for the cases of sources above or under other planes (e.g., $x = x_0$). Since it is possible to enclose the block by a surface with flat faces, then the field outside can be expanded by employing a plane-wave expansion for each face of the enclosing surface.

In order to illustrate it, let us consider the two-dimensional case depicted in Figure 2. In this example, the body is enclosed by a rectangle so that the sources can be decomposed into four groups. The first and second groups are the sources above and under the rectangle, re-spectively, whereas the third and four groups are the sources at the right and left of the rec-tangle which do not belong to any of the previous groups. Thus, it is possible to carry out expansions similar to the one in (7) for each plane and, therefore, to express the field inside the rectangle as a superposition of plane-waves.
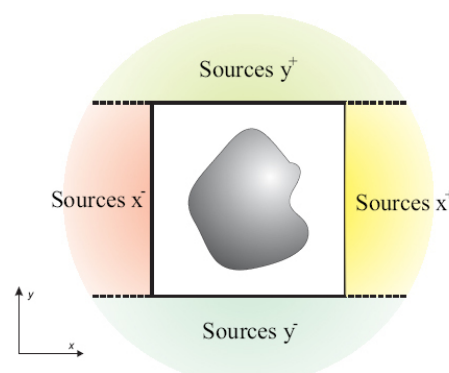


**Figure 2.** Decomposition of the outer sources into regions for the expansion into plane-waves.

The PWS is *infinite* and *unbounded* as inferred from (7). Hence, several numerical approxima-tions must be carried out. The first one consist on sampling the PWS; guidelines to choose the number of plane-waves depending on the electrical size of the block are given in [28].

In order to truncate the PWS, it is important to observe that it can be split into two regions. The visible region corresponds to the area where the propagation vector is real and, therefore, the wave propagates in that direction. On the other hand, the invisible region corresponds to propagation vectors where at least one of the components is complex and, therefore, this kind of waves is attenuated when it travels away from the sources. Thus, if we assume that the block is far enough from the sources, then it is possible to neglect the contribution from the invisible spectrum. Similar approximations for the PWS were carried out for the analysis of open cavities in [41].

If the blocks are close (or touching each other), then the approximation of neglecting the invisible spectrum can slow down the convergence of the solution in terms of the number of the CBFs. In order to overcome it, when illuminating with plane-waves, the blocks are not considered isolated. Instead of that, they are solved together with a small portion of the continuous blocks. Typical block extensions are between $0.1\lambda$ and $\lambda$.

Taking into account these two approximations, the coefficients for the CBFs can be computed as:

$$\overline{\overline{Z}}_{ii}\widetilde{\overline{J}}'_i = \overline{\overline{V}}_i \quad by\ i=1,\ ...,\ M \tag{9}$$

where is the matrix containing the field tested by the basis functions in the extended $i$-th block due to each plane waves. Each column of the matrix corresponds to an excitation vector and, therefore, its dimensions are $\widetilde{N}_i \times N_{PW}$, where $\widetilde{N}_i$ is the number of low-level basis functions in the extended block and $N_{PW}$ is the number of considered plane-waves.

After discarding the currents on the extensions, a complete set of basis functions, $\widetilde{\overline{J}}'_i$, is achieved. Nonetheless, the linear dependency of these CBFs is not warranted and, hence, if they were used as basis functions, it would yield a MoM matrix that could be ill-conditioned or even singular. In order to detect the number of degrees of freedom in the matrix $\widetilde{\overline{J}}'_i$, a *singular value decomposition* (e.g., see [16]) is used. This factorization yields the following result:

$$\overline{\overline{J}}'_i = \overline{\overline{U}}_i\overline{\overline{D}}_i\overline{\overline{W}}_i \tag{10}$$

where $\overline{\overline{W}}_i$ and $\overline{\overline{U}}_i$ are orthogonal matrices with dimensions $N_i \times N_i$ and $N_{PW} \times N_{PW}$, where as $\overline{\overline{D}}_i$ is a diagonal matrix with dimensions $N_i \times N_{PW}$ that contains the singular values $\sigma$. It will be assumed that the singular values in the diagonal of $\overline{\overline{D}}_i$ are arranged from the highest one to the smaller one without loss of generality.

The columns of $\overline{\overline{U}}_i$ are orthogonal each other and, therefore, they are a complete base of the vector subspace generated by the column vectors in $\overline{\overline{U}}_i$. In addition, the ratio $\sigma_k/\sigma_1$ is a measurement of the dependency of the $k$-column of $\overline{\overline{U}}_i$ with respect to the first $k-1$ first columns. Hence, if the singular values under a given threshold are approximated by zero,

then it is only necessary to retain the columns in $\overline{\overline{U}}$ with the singular values over the previous threshold. Finally, the matrix containing the coefficients by columns of the CBFs is:

$$\overline{\overline{J}}_i = \overline{\overline{U}}_i(:, 1:K_i) \tag{11}$$

where $K_i$ is the number of singular values normalized by $\sigma_1$ that are over a given threshold $t_{svd}$. The Matlab [36] notation $U_i(:, 1:K_i)$ denotes all the columns in $U_i$ from the first one to the $K_i$-th one.

The inclusion of the SVD provides an efficient way to compute CBFs that are independent each other and, furthermore, it enables an adjust of the quality of the solution by means of the threshold $t_{svd}$. On the contrary, one of the drawbacks of employing a SVD is that the CBFs lose the physical meaning since they do not correspond anymore to the currents induced by each plane-wave but they are a linear combination of them.

## 2.3 Reduced matrix computation

In the CBFM, the coefficients of the matrix of the system of equations are the reaction terms between CBFs. Thus, considering the EFIE, the Galerkin's method and a symmetric product for the testing, then the reaction term between the $m$-th basis function in the $i$-th block and the $n$-th basis function in the $j$-th block is given by:

$$\overline{\overline{Z}}_{ij}^{(1)}(m, n) = \left\langle \mathcal{F}_{i,m}, \mathcal{L}\left(\mathcal{F}_{j,n}\right) \right\rangle, \tag{12}$$

where the index (1) denotes that the matrix contains the interaction between the CBFs instead of the interaction between low-level basis functions. This superindex will be deeply exploited when considering the multilevel version of the CBFM.

If (3) is introduced in (12):

$$\overline{\overline{Z}}_{ij}^{(1)}(m, n) = \sum_{p=1}^{N_i} \sum_{q=1}^{N_j} I_{i,p}^{(m)} I_{j,q}^{(n)} \left\langle \mathbf{f}_{i,p}, \mathcal{L}\left(\mathbf{f}_{j,q}\right) \right\rangle = \sum_{p=1}^{N_i} \sum_{q=1}^{N_j} I_{i,p}^{(m)} I_{j,q}^{(n)} \overline{\overline{Z}}_{ij}^{(0)}(p, q)$$

$$= \left[ I_{i,1}^{(m)} \; I_{i,2}^{(m)} \; \cdots \; I_{i,N_i}^{(m)} \right] \cdot \overline{\overline{Z}}_{ij}^{(0)} \cdot \begin{bmatrix} I_{j,1}^{(m)} \\ I_{j,2}^{(m)} \\ \vdots \\ I_{j,N_j}^{(m)} \end{bmatrix}, \tag{13}$$

where $\overline{\overline{Z}}_{ij}^{(0)}$ is the matrix that contains the reaction terms between the low-level basis functions in the $i$-th observation block and the $j$-th source block.

Equation (13) enables us to express the reaction terms between the CBFs of two blocks as a simple product between matrices:

$$\bar{\bar{Z}}_{ij}^{(1)} = \bar{\bar{J}}_i^T \, \bar{\bar{Z}}_{ij}^{(0)} \, \bar{\bar{J}}_j \tag{14}$$

where $\bar{\bar{Z}}_{ij}^{(1)}$ is the matrix containing the reaction terms between the CBFs in the $i$-th observation block and $j$-th source block.

The matrix of the system of equations for the CBFM, $\bar{\bar{Z}}^{(1)}$, is usually referred to as the *reduced matrix* and it can be computed by means of matrix-matrix products involving the coefficients of the CBFs and the reaction terms of the low-level basis functions:

$$\bar{\bar{Z}}^{(1)} = \begin{bmatrix} \bar{\bar{J}}_1^T \bar{\bar{Z}}_{11}^{(0)} \bar{\bar{J}}_1 & \bar{\bar{J}}_1^T \bar{\bar{Z}}_{12}^{(0)} \bar{\bar{J}}_2 & \cdots & \bar{\bar{J}}_1^T \bar{\bar{Z}}_{1B}^{(0)} \bar{\bar{J}}_B \\ \bar{\bar{J}}_2^T \bar{\bar{Z}}_{21}^{(0)} \bar{\bar{J}}_1 & \bar{\bar{J}}_2^T \bar{\bar{Z}}_{22}^{(0)} \bar{\bar{J}}_2 & \cdots & \bar{\bar{J}}_2^T \bar{\bar{Z}}_{2B}^{(0)} \bar{\bar{J}}_B \\ \vdots & \vdots & \ddots & \vdots \\ \bar{\bar{J}}_B^T \bar{\bar{Z}}_{B1}^{(0)} \bar{\bar{J}}_1 & \bar{\bar{J}}_B^T \bar{\bar{Z}}_{B2}^{(0)} \bar{\bar{J}}_2 & \cdots & \bar{\bar{J}}_B^T \bar{\bar{Z}}_{BB}^{(0)} \bar{\bar{J}}_B \end{bmatrix}. \tag{15}$$

It is important to remark that the computation of the reduced matrix involves the entire MoM matrix. Nonetheless, it is not necessary to store the entire matrix in memory at the same time. Instead of that, it is only required to store the block of the original MoM matrix that is employed for the computation of each submatrix in the reduced matrix.

Similar steps can be followed in order to computed the feeding vector (or feeding matrix if multiple excitations are considered) by means of the following expression:

$$\bar{\bar{V}}^{(1)} = \begin{bmatrix} \bar{\bar{J}}_1^T \bar{\bar{V}}_1^{(0)} \\ \bar{\bar{J}}_2^T \bar{\bar{V}}_2^{(0)} \\ \vdots \\ \bar{\bar{J}}_B^T \bar{\bar{V}}_B^{(0)} \end{bmatrix} \tag{16}$$

where $V_i^{(0)}$ is the feeding matrix containing the low-level feeding vectors of the $i$-th block.

### 2.3.1 Fast computation of the reduced matrix

Since the reduced matrix involves all the terms in the MoM matrix, the computational times can be considerably high for electrically large problems. Several approaches are available in the literature to mitigate this drawback. One of the most successful approaches has been the one presented in [10] for the fast computation of reaction terms between the CBFs of an array of repeated elements. This method is based on a *multipolar expansion* of the free space Green's function as in the FMM.

Another method is the one presented in [34] based on the *adaptive cross approximation* (ACA) [2,3]. In this method, the matrices containing the reaction terms between two blocks are

modeled by a matrix product of two matrices that can be efficiently computed. In addition, this efficiency improves with the distance between blocks.

A third technique has been proposed in [30]. In this approach, the field radiated by the CBFs of a source block is computed on the observation block by carrying out an interpolation so that it avoids integrating the currents on the source block for each point of the observation block.

Table 1 contains a comparison of the main characteristic of these methods. The points that have been considered are the following ones:

| | ACA | Multipolar expansion | Interpolation |
|---|---|---|---|
| Setup time | ✓ | X | ✓ |
| Additional memory requirements | ✓ | X | ✓ |
| Dependency on the Green''s function | ✓ | X | ✓ |
| Distance adaptation | ✓ | X | ✓ |
| Continuous blocks | – | X | ✓ |
| Arbitrarily-shaped blocks | ✓ | ✓ | X |

Table 1. Comparison of several fast methods for computing the reaction terms between CBFs.

- Setup time: the multipolar expansion requires the precomputation of certain parameters. On the hand, the interpolation scheme and the ACA does not require this step.

- Additional memory requirements: the precomputations carried out by the multipolar expansion on the setup stage must be kept in memory so that introduces an additional penalty that does not exist in the other methods.

- Dependency on the Green's function: the ACA and interpolation scheme does not depend on the Green's function that is considered (e.g., free space, multilayer, periodic structure, etc.). Nevertheless, different formulations of the multipolar scheme have to be considered depending on the Green''s function.

- Distance adaptation: the ACA becomes faster depending on the distance between the blocks. Similarly, the interpolation scheme reduces the number of evaluation points so that it also becomes faster if the distance between source and observation blocks is increased. The conventional multipolar expansion does not provide a mechanism to take advantage of the distance between the blocks.

- Contiguous blocks: multipolar expansion can only be applied to blocks in the far-field so that it is not used for contiguous blocks. Although, the interpolation scheme and the adaptive cross approximation can work for contiguous blocks, it results not so efficient for these blocks due to a considerable slowdown of the computations.

- Arbitrary-shaped blocks: the interpolation scheme is designed for planar blocks and, therefore, it only works for two-dimensional blocks.

According to the previous considerations, the ACA seems to be the most complete and versatile method for the combination of it with the CBFM. Thus, it will be used in the rest of the paper for the computation of the reduced matrix unless otherwise indicated.

### 2.4 Solution of the system of equations

Once the matrix and feeding vector have been computed, the following system of equations must be solved:

$$\bar{\bar{Z}}^{(1)}\bar{I}^{(1)} = \bar{V}^{(1)} \tag{17}$$

where $I^{(1)}$ is the vector containing the unknowns for the expansion of the currents in (2): and $I_i^{(1)}$ are the coefficients of the expansions of the CBFs in the $i$-th block:

$$\bar{I}^{(1)} = \begin{bmatrix} \bar{I}_1^{(1)} \\ \bar{I}_2^{(1)} \\ \vdots \\ \bar{I}_B^{(1)} \end{bmatrix} \tag{18}$$

and $I_i^{(1)}$ are the coefficients of the expansions of the CBFs in the $i$-th block:

$$\bar{I}_i^{(1)} = \begin{bmatrix} I_1^{(1)} \\ I_2^{(1)} \\ \vdots \\ I_{i,\,N_i} \end{bmatrix} \tag{19}$$

Once (17) has been solved, it is possible to retrieved the currents vector for the low-level basis functions by expanding the coefficients of the CBFs:

$$\bar{I} = \begin{bmatrix} \bar{\bar{J}}_1 I_1^{(1)} \\ \bar{\bar{J}}_2 I_2^{(1)} \\ \vdots \\ \bar{\bar{J}}_B \bar{I}_B^{(1)} \end{bmatrix} \tag{20}$$

If multiple excitations are considered, then $\widetilde{V}^{(1)}$ becomes a matrix a previously dis-cussed. As a consequence, $\tilde{I}^{(1)}$ become also a matrix containing the solution for each ex-citation on each column.

## 2.5 Nested characteristic basis functions

The most important feature of the CBFM is the capacity to solve a problem with a number of unknowns smaller than the number required by the conventional MoM. It has been empiri-cally proved that the compression rate of the CBFM (i.e., the ratio of the number of low-level basis functions to CBFs) increases if the size of the blocks is increased. Figure 3 shows that the number of CBFs that survives to the SVD filtering does not have a linear behavior with the surface and, therefore, it is always recommended to consider blocks as electrically large as possible to improve the compression.
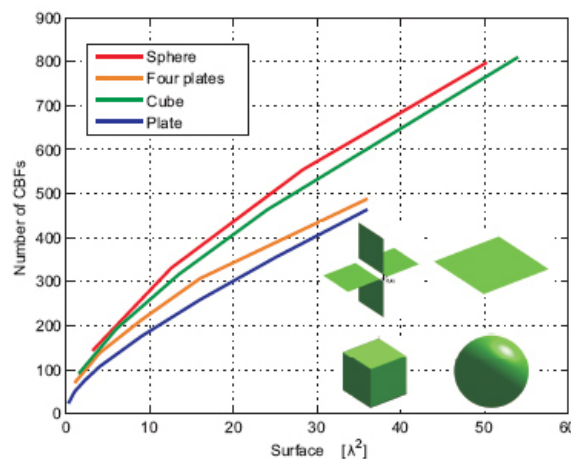


**Figure 3.** Number of required CBFs for different surfaces as a function of the electrical size.

However, the main drawback of increasing the size of the blocks is that the computation of the CBFs requires more computational resources to solve (9). In order to alleviate this task, a possible alternative is to split the blocks into sublocks and, thus, applied the CBFM to solve (9). Hence, it results into a *recursive scheme* where the CBFs can be expressed in terms of CBFs from a lower level.

The first step to apply the multilevel CBFM (ML-CBFM) is to hierarchically decompose the geometry into blocks until reaching the low-level basis functions. A decomposition example is shown in Figure 4 for a two level decomposition of the NASA almond.
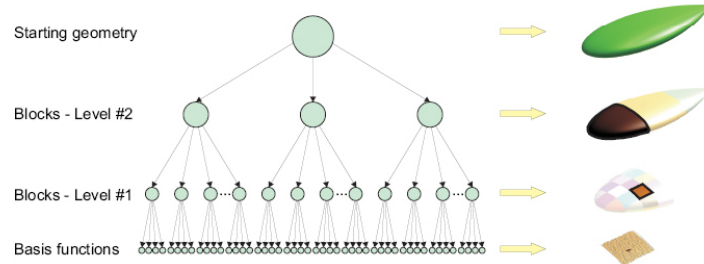
**Figure 4.** Hierarchical decomposition of the geometry.

In order to mathematically express the multilevel formulation, it is useful to define the notation for a *sequence of blocks* $\{seq\}=\{i_1, i_2, \ldots, i_l\}$ where the values $i_k$ are the indexes of the blocks from the highest level to the lower one. Thus, $\{seq\}=\{2, 5\}$ is used to denote the fifth block, which belongs to the first level, of the second block, which belongs to the second and highest level.

Thus, the $n$-th CBF inside the block $\{seq\}$ is given by:

$$\mathcal{F}_{\{seq\},n} = \sum_{b=1}^{B_{\{seq\}}} \sum_{m=1}^{N_{\{seq,b\}}} I_{\{seq,b\},m}^{(n)} \mathcal{F}_{\{seq,b\},m}, \tag{21}$$

where $B_{\{seq\}}$ is the number of block inside the block pointed by $N_{\{seq,b\}}$ is the number of CBFs in the block $I_{\{seq,b\},m}^{(n)}$ are the coefficients for the expansion in terms of the CBFs on the supporting sublocks. The CBFs from the first level, i.e., the level before the low-level basis functions, are defined as in the single-level CBFM in terms of the low-level basis functions:

$$\mathcal{F}_{\{seq\},n} = \sum_{m=1}^{N_{\{seq\}}} I_{\{seq\},m}^{(n)} \mathbf{f}_{\{seq\},m}. \tag{22}$$

The current is as usually expressed as a linear combination of the highest level CBFs:

$$\mathbf{J} = \sum_{b=1}^{B} \sum_{m=1}^{N_{\{b\}}} I_{\{b\},m} \mathcal{F}_{\{b\},m}, \tag{23}$$

where $B$ is the number of blocks and $I_{\{b\},m}$ are the coefficients to be computed by solving the system of equations of the MoM.

The computation of the coefficients of the CBFs for each level is carried out in a similar fashion to the monolevel CBFM. Firstly, the first level blocks are illuminated by multiple plane-

waves and the CBFs are obtained on them by computing the currents and applying the SVD filter. Next, the second level blocks are again illuminated by multiple plane-waves and the induced currents (expressed in terms of the first level CBFs) are computed and filtered out. The procedure is repeated until reaching the highest level. It is important to note that the number of plane-waves and the SVD threshold can be different for each level depending on the required accuracy.

Once the CBFs for each block in the highest level have been computed, then it is possible to compute the system of equations matrix containing the reaction terms by applying again a nested scheme. The reaction terms between the CBFs of the ($I$ - 1)-th level belonging to the blocks {d} and {e} of the ($I$-1)-th level level can be expressed as:

$$
\overline{\overline{Z}}^{(l-1)}_{\{d\},\{e\}} = \begin{bmatrix}
\overline{\overline{Z}}^{(l-1)}_{\{d,1\},\{e,1\}} & \overline{\overline{Z}}^{(l-1)}_{\{d,1\},\{e,2\}} & \cdots & \overline{\overline{Z}}^{(l-1)}_{\{d,1\},\{e,1\}} \\
\overline{\overline{Z}}^{(l-1)}_{\{d,2\},\{e,1\}} & \overline{\overline{Z}}^{(l-1)}_{\{d,2\},\{e,2\}} & \cdots & \overline{\overline{Z}}^{(l-1)}_{\{d,2\},\{e,B_{(e)}\}} \\
\vdots & \vdots & \ddots & \vdots \\
\overline{\overline{Z}}^{(l-1)}_{\{d,B_{\{d\}}\},\{e,1\}} & \overline{\overline{Z}}^{(l-1)}_{\{d,1\},\{e,1\}} & \cdots & \overline{\overline{Z}}^{(l-1)}_{\{d,B_{\{d\}}\},\{e,B_{(e)}\}}
\end{bmatrix},
\tag{24}
$$

where each submatrix can be computed by considering the coefficients of the CBFs definition and the reaction terms from the CBFs of the previous level:

$$
\overline{\overline{Z}}^{(l)}_{\{d\},\{e\}} = \overline{\overline{J}}^{T}_{\{d\}} \overline{\overline{J}}^{(l-1)}_{\{d\},\{e\}} \overline{\overline{J}}_{\{e\}}.
\tag{25}
$$

Similar steps can be carried out to compute the feeding vector (or matrix in the case of multiple excitations) so that the following system of equations can be solved in order to find the unknown coefficients in (23):

$$
\overline{\overline{Z}}^{(L)} \overline{I}^{(L)} = \overline{V}^{(L)}.
\tag{26}
$$

Once the system of equations has been solved, it is possible to express the CBFs in terms of the CBFs of the next level by means of the following operation:

$$
\begin{bmatrix}
\overline{I}^{(l-1)}_{\{seq,1\}} \\
\overline{I}^{(l-1)}_{\{seq,2\}} \\
\vdots \\
\overline{I}^{(l-1)}_{\{seq,B_{\{seq\}}\}}
\end{bmatrix} = \overline{\overline{J}}_{\{seq\}} \overline{I}^{(l)}_{\{seq\}}
\tag{27}
$$

this formulation can be applied to all the blocks and repeated until reaching the lowest level so that the solution is expressed in terms of the conventional low-level basis functions.

In the case of considering multiple excitations, the vectors $V^{(L)}$, and the equivalent vectors for each level, becomes matrices as discussed in the single-level CBFM

# 3. Applications

As it has been shown in the previous sections, the CBFM enables to comprise the MoM matrix. Since the solution of the system of equations is the most time consuming stage for the analysis of electrically large problems with the MoM, a reduction of the number of unknowns will significantly decrease the *total solution time*. Furthermore, the factor limiting the size of the problems that can be solved with the conventional MoM is size of the impedance matrix which must fit in the available RAM memory. Thus, the CBFM compression results on an *extension of the application range* of the MoM. Considering these two facts, the CBFM can be considered a *speed-up technique for the MoM*. In addition, the CBFM is not based on an iterative scheme so it will not suffer from converge problems.

Although the use of the CBFM to compute an iteration-free of relatively large problems may be the most direct application of the MoM, it will be shown in the following sections that the compression of the MoM matrix can be exploited for many other purposes.

## 3.1 Monostatic Radar Cross Section Computation

The compressed system of equations described by (17) and (26) for the monolevel- and multilevel-CBFM, respectively, can be solved by using conventional direct solutions schemes such as a LU decomposition for problems electrically larger than the ones that can be solved by the MoM. These schemes can handle a relatively large number of RHS with a negligible time increment with respect of the case with a single RHS. As a consequence, many authors (e.g., [33,11]) have benefited from this advantage to compute monostatic radar cross sections (RCS) where there are as many RHS as incident angles.

This application is illustrated for the computation of the monostatic RCS of a $4\lambda$ cube. The cube is solved with a single level CBFM by decomposing the geometry into 24 blocks of size $2\lambda \times 2\lambda$ (see Figure 5). The number of plane waves to solve the problem is 400 and the SVD threshold is set to $10^{-3}$. The original problem was discretized into 31728 RWG unknowns that were reduced to only 3004 after applying the CBFM.

The results for the $\theta - \theta$ RCS for 91 points in the cut $\phi = 0$ are shown in Figure 5 together with the reference results from the MoM. Excellent agreement is found between both of them.
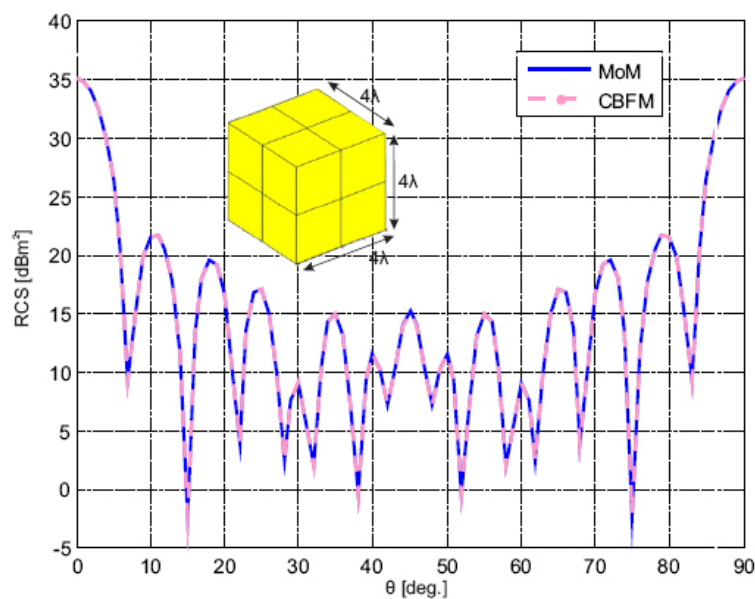
**Figure 5.** Monostatic RCS for a 4λ cube computed by the MoM and the CBFM.

The CPU times are shown in Table 2. In this case, the ACA has not been used to speed-up the matrix filling time which is the most time consuming stage. The CPU times for the CBFM simulation have been computed on a PC equipped with an Intel® Core™ at 2.4 GHz (only one core was used) and 4GB RAM memory whereas the MoM simulation was run on a computational server in order to fit the impedance matrix on the RAM memory. This server is equipped with 8 Dual Core AMD Opteron™ 880 at 2.4GHz (only one core was used) and 56GB of RAM.

|  | CBFs generation | Matrix filling time | Solving time | Total time |
| --- | --- | --- | --- | --- |
| MoM | - | 1468s | 14198s | 15666s |
| CBFM | 510s | 1614s | 14s | 2138s |

**Table 2.** Computational times for solving a 4λ cube with the MoM and the CBFM.

Although the size of the previous problem is relatively electrically small, it shows how the compression of CBFM enables to solve problems larger than the ones solved by the conventional MoM. The solution of larger problems can be efficiently carried out by combining the multilevel scheme together with an appropriate parallelization scheme [29].

### 3.2 Fast evaluation of phased arrays

In addition to the monostatic RCS computation, there are other cases where the simultaneous solution of multiple RHS is highly recommended. One important example is the synthe-

sis of phased arrays. In this problem, the optimal combination of voltages at the input of each element of the array has to be found in order to achieved the desired radiation pattern. It is possible to show [1] that there is a matrix, $\bar{\bar{G}}$, that relates the samples of the electromagnetic field on a given set of points (e.g., a circular cut of points in the far-field) with the voltages by the following matrix-vector product:

$$\bar{E} = \bar{\bar{G}}\bar{v} \tag{28}$$

Once this matrix has been obtained, then the computation of the radiated field for a certain choice of voltages can be computed with a very small computational effort. Nonetheless, the computation of this matrix involves solving the geometry of the entire problem (the array and the surrounding elements) for as many RHS as elements [1]. Therefore, the computation of $\bar{\bar{G}}$ can be very time-consuming when the number of elements in the array is high and the structure to be solved is electrically large. As in the previous example, the CBFM can help to mitigate the computational cost due to its ability to solve simultaneously multiple RHS.

In order to illustrate this example, a secondary surveillance radar (SSR) is considered. In this kind of problems, it is very important to have a low level of secondary lobes to avoid false interrogations. The radar under analysis consist on an array of 10×33 elements that is surrounded by the supporting structure, a primary radar, a circular supporting platform and several lighting rods (see Figure 6). The working frequency is 1030 MHz so that the geometry is discretized into 139, 762 RWGs.
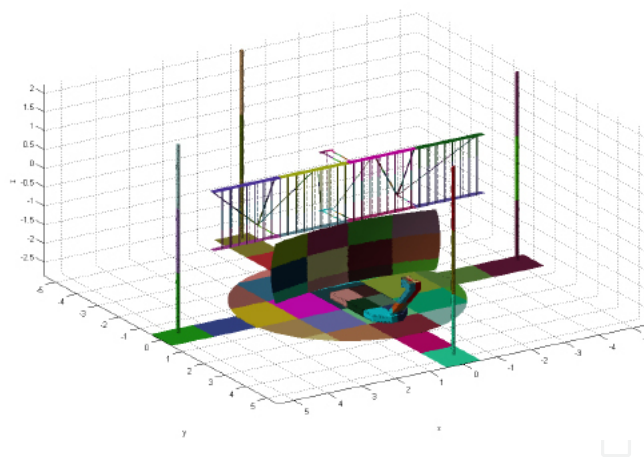


**Figure 6.** First level decomposition for a secondary surveillance radar.

A two level CBFM is used to efficiently compute the matrix in (28). The first level blocks are shown in Figure 6. After applying an SVD threshold equal to $10^{-3}$, the number of first-level CBFs is only 20259.

A second level CBFM is applied on this first-level CBFs by grouping the blocks into five macro blocks. The first one contains the SSR and the supporting structure, and the remaining four blocks contain the rest of the structure. The number of degrees of freedom after this

second level is reduced to 13312. In both cases, the number of plane waves to illuminates the first- and second-level blocks is 6720.

In this example, a separable distribution of the feedings is assumed and, therefore, the elevation and azimuth radiation patterns are assumed to be controlled by the feeding distribution on the vertical and horizontal distribution. The vertical distribution is designed as in [25] which considers the isolated structure and computes the vertical feeding to provide a cosecant squared pattern. On the other hand, the azimuth elevation pattern, which must suit the masks depicted in Figure 7, is expected to be affected by the surrounding environment and, in special, by the lighting rods. Thus, the feedings computed in [25] are not expected to be valid and they must be synthesized for the new structure. Hence, the matrix G has been computed to relates the 33 voltages of the horizontal distribution with 181 sample points of the azimuth radiation pattern.

Once the matrix is computed, many synthesis schemes can be efficiently applied. In this book chapter, a genetic algorithm has been used to generated the proper radiation pattern shown in Figure 7 but other optimization techniques could also be used [26]. The evaluation of each generation of the genetic algorithm, which involves computing a hundred of radiation pattern, is accomplished in only 0.22 seconds. In opposite, the radiation pattern of a usual hamming window distribution is also shown revealing that it is out of the mask.
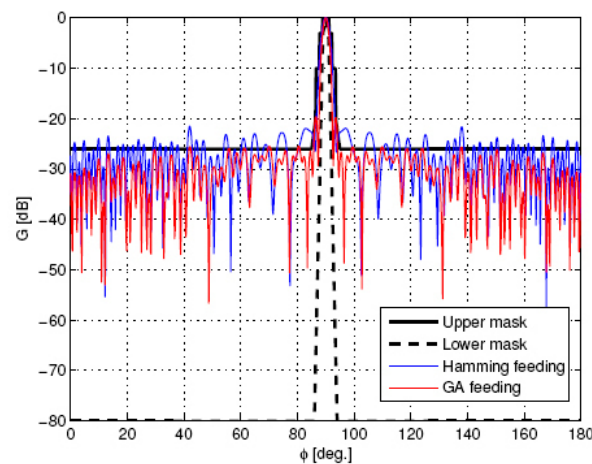


**Figure 7.** Normalized radiation patterns for a hamming window feeding and a feeding computed by a genetic algorithm.

### 3.3 Partial modifications for the analysis of on-board antennas

The quick expansion of iterative schemes such as the fast multipole method has enabled us to solve problems electrically larger than in the past. Nonetheless, some enhancements of the MoM cannot be easily applied on these iterative schemes. Since the CBFM is an extended version of the MoM in which the conventional low-level basis functions are replaced by CBFs, then most of MoM enhancements can be easily adapted.

The partial solution of geometries [23,37,21,9] is one of these approaches that can be easily applied to the CBFM. In this book chapter, we will focus on the partial solution based on the Sherman-Morrison formula as described in [24].

In this technique, the structure is splitted into two parts. The first one is assumed to be fixed and it will not be modified. The other part is assumed to be smaller than the first one and it is assumed that it needs to be modified several times during the analysis. Thus, once the fixed geometry is known, it is possible to carry out most of the steps to compute the inverse of the entire impedance matrix so that the analysis of each modification can be resumed from that point saving computational effort. Since the inverse of the entire matrix is involved, then it can only be applied to problems where this matrix fits in the available RAM memory and, hence, the CBFM extends the range of applicability of the method to geometries electrically larger than the structures analyzed by the conventional MoM.

An example of application of these techniques could be the analysis of an antenna on an airplane affected by the turbines rotation. In this problem, the airplane must be solved for different rotation angles of the turbines in order to check the impact of them in the radiation characteristics of it. In this case, the fixed structure would be the airplane without the turbines what comprises most of the total geometry, and the turbines areas are the parts that must be modified.

In this book chapter, the technique is illustrated for a problem similar to the previously described where the analysis of the radiation pattern of an monopole placed on an helicopter affected by the blades rotation is accomplished. The geometry is shown in Figure 8 and the monopole is placed at the beginning of the tail and parallel to it. The problem is solved at 400, MHz so that the geometry is discretized into 96, 851 low-level basis functions. After the application of the CBFM with 400 plane waves and a SVD threshold equal to $10^{-3}$, the number of degrees of freedom for the total problem is 9837 with only 830 belonging to the blades.

The analysis of the structure with the CBFM involves 10, 200 s. On the other hand, the required precomputations with the technique described in this section requires 10, 026 s. After that, the analysis of each new blades position can be accomplished in only 865s. Thus, the analysis with this technique becomes quickly more efficient than the use of the conventional CBFM. Times are measured in a machine equipped with four Quad-Core AMD Opteron™ 8378 at 2.4 GHz (only one core was used) and 128 GB of RAM. The radiation patterns for several rotation angles of the main rotor are shown in Figure 8.

Finally, it is important to remark that other approaches can be used for similar purposes. For example, antenna placement is considered in [27] by combining the CBFM with an incomplete Gauss-Jordan elimination.
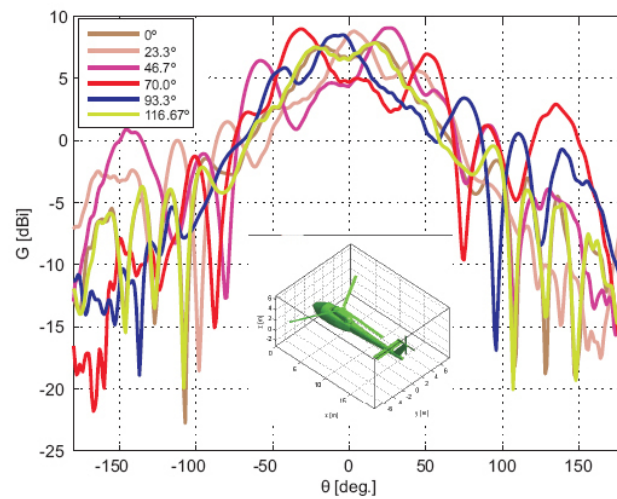
**Figure 8.** Gain on the cut =90° for different rotation positions in the main rotor. The inset depicts the helicopter with the blades at the zero angle.

## 4. Conclusions

The characteristic basis function method has been deeply described in this book chapter. New perspectives have been provided to understand the generation of the characteristic basis functions based on plane-waves revealing that it yields a complete set of basis functions if the approximation of external field is accurate enough. Several speeds up have been compared for the case of filling the impedance matrix and the adaptive cross approximation seems to be the most balanced one for a generic analysis.

As a consequence, the CBFM has been proved to be a rigorous method that achieved an iteration-free solution for problems electrically larger than the ones that can be analyzed with the conventional method of moments. In addition, the compression of the matrix that the CBFM carries out is compatible with many of the MoM enhancements. The most direct application is the solution of problems where multiple excitations have to be considered such as monostatic radar cross section computations or characterization of antenna arrays. In addition, techniques for efficiently analysis of small modifications on large structures have been shown to be compatible with the CBFM.

## 5. Acknowledgments

## Author details

Jaime Laviada[*], Fernando Las-Heras and Marcos R. Pino

*Address all correspondence to: jlaviada@tsc.uniovi.es

Escuela Politécnica de ingeniería de Gijón, Universidad de Oviedo, Electrical Engineering Department, Gijón, España

## References

[1] Ayestarán, R.G., Laviada, J., & Las-Heras, F. (2009). Realistic antenna array synthesis in complex environments using a MoM-SVR approach. *J. of Electromagn. Waves and Appl.*, 23, 97-108.

[2] Bebendorf, M. (June 2000). Approximation of boundary element matrices. *Numen. Math*, 86(4), 565-589.

[3] Bebendorf, M., & Rjasanow, S. (March 2003). Adaptive low-rank approximation of collocation matrices. *Computing*, 70(1), 1-24.

[4] Bilotti, F., & Vegni, C. (December 2001). Rigorous and efficient full-wave analysis of trapezoidal patch antennas. *IEEE Trans. Antennas Propagat.*, 49(12), 1773-1776.

[5] Bleszynski, E., Bleszynski, M., & Jaroszewicz, T. (Sep.-Oct. 1996). AIM: adaptive integral method for solving large-scale electromagnetic scattering and radiation problems. *Radio Sci.*, 31(5), 1225-1251.

[6] Cabedo-Fabres, M., Antonino-Daviu, E., Valero-Nogueira, A., & Bataller, M. F. (October 2007). The theory of characteristic modes revisited: A contribution to the design of antennas for modern applications. *IEEE Antennas Propagat. Mag.*, 49(5), 52-68.

[7] Chew, W. C., Jin, J. M., Michielssen, E., & Song, J. (2001). Fast and efficient algorithms in computational electromagnetics. Artech House, Norwood, Massachusetts 02062, USA.

[8] Coifman, R., Rokhlin, V., & Wandzura, S. (June 1993). The fast multipole method for the wave equation: A pedestrian prescription. *IEEE Trans. Antennas Propagat. Mag.*, 53(3), 7-12.

[9] Cormos, D., Loison, R., & Gillard, R. (June 2005). Fast optimization and sensitivity analysis of nonintuitive planar structures. *IEEE Trans. Microwave Theory Tech.*, 53(6), 2019-2025.

[10] Craeye, Christophe. (October 2006). A fast impedance and pattern computation scheme for finite antenna arrays. *IEEE Trans. Antennas Propagat.*, 54(10), 3030-3034.

[11] Delgado, Carlos, Felipe Cátedra, Manuel, & Mittra, Raj. (March 2008). Application of the characteristic basis function method utilizing a class of basis and testing functions defined on NURBS patches. *IEEE Antennas Propagat.*, 56(3), 784-791.

[12] Eshrah, Islam A., & Kishk, Ahmed A. (June 2004). Application of the adaptive basis functions/diagonal moment matrix technique to arrays of dielectric scatterers. *Proc. IEEE AP-S Int. Symp.*, 1, 647-650.

[13] Eshrah, Islam A., & Kishk, Ahmed A. (May 2004). Implementation of the adaptive basis functions/diagonal moment matrix technique to array of identical elements. *Proc. URSI International Symposium on Electromagnetic Theory*, 837-839.

[14] Eshrah, Islam A., & Kishk, Ahmed A. (March 2005). Analysis of linear arrays using the adaptive basis functions/diagonal moment matrix technique. *IEEE Trans. Antennas Propagat.*, 53(3), 1121-1125.

[15] Glisson, A. W., & Wilton, D. R. (September 1980). Simple and efficient numerical methods for problems of electromagnetic radiation and scattering from surfaces. *IEEE Trans. Antennas Propagat.*, AP-28(5), 593-603.

[16] Golub, G. H., & Loan, C. F. van. (1989). Matrix computations. John Hopkins Univ. Press, Baltimore, MD.

[17] Hansen, T. B., & Yaghjian, Arthur D. (1999). Plane-Wave Theory of time domain fields. IEEE press, New York, NY.

[18] Harrington, R. F., & Mautz, J. R. (September 1971). Computation of characteristic modes for conducting bodies. *IEEE Trans. Antennas Propagat.*, AP-19, 629-639.

[19] Harrington, R. F., & Mautz, J. R. (September 1971). Theory of characteristic modes for conducting bodies. *IEEE Trans. Antennas Propagat.*, AP-19, 622-628.

[20] Harrington, R.F. (1993). Field Computation by Moment Method. IEEE press, New York, NY.

[21] Johnson, J. Michael, & Rahmat-Samii, Yahya. (October 1999). Genetic algorithms and method of moments ({GA/MOM}) for the design of integrated antennas. *IEEE Trans. Antennas Propagat.*, 47(10), 1606-1614.

[22] Kalbasi, Khalil, & Demarest, Kenneth R. (May 1993). A multilevel formulation of the method of moments. *IEEE Trans. Antennas Propagat.*, 41(5), 589-599.

[23] Kastner, R. (March 1989). An 'add-on' method for the analysis of scattering from large planar structures. *IEEE Trans. Antennas Propagat.*, 37(3), 353-361.

[24] Kastner, R. (January 1990). Analysis of microstrip antenna structures using the 'add-on' technique. *IEEE Trans. Antennas Propagat.*, 38(1), 114-117.

[25] Las-Heras, F., Galocha, B., & Besada, J. L. (July 1997). Equivalent source modelling and reconstruction for antenna measurement and synthesis. *Proc. IEEE AP-S Int. Symp.*, 1, 156-159, Montreal, Canada.

[26] Laviada, J., Ayestarán, R.G., Pino, M. R., Las-Heras, F., & Mittra, R. (2009). Synthesis of phased arrays in complex environments with the multilevel characteristic basis function method. *Progress In Electromagnetics Research*, 92, 347-360.

[27] Laviada, J., Gutiérrez-Meana, J., Pino, M. R., & Las-Heras, F. (October 2010). A partial solution of MoM matrices based on characteristic basis functions and its application to on-board antennas positioning. *Applied Computational Electromagnetics Society (ACES) Journal*, 25(10), 830-840.

[28] Laviada, J., Pino, M. R., Las-Heras, F., & Mittra, Raj. (October 2009). Solution of electrically large problems with multilevel characteristic basis functions. *IEEE Trans. Antennas Propagat.*, 57(10), 3189-3198.

[29] Laviada, J., Pino, M. R., Mittra, R., & Las-Heras, Fernando. (December 2009). Parallelized multilevel characteristic basis function method for solving electromagnetic scattering problems. *Microwave Optical and Technology Letters*, 51(12), 2963-2969.

[30] Laviada, J., Pino, Marcos R., Las-Heras, F., & Mittra, R. (August 2009). Interpolation scheme for fast calculation of reaction terms in the characteristic basis function method. *Microwave Optical and Technology Letters*, 51(8), 1818-1824.

[31] Losada, V., Boix, R. R., & Horno, M. (April 1999). Resonant modes of circular microstrip patches in multilayered substrates. *IEEE Trans. Antennas Propagat.*, 47, 488-498.

[32] Wei Bing, Lu, Cui, Tie Jun, Qian, Zhi Guo, Yin, Xiao Xing, & Hong, Wei. (November 2004). Accurate analysis of large-scale periodic structures using an efficient sub-entire-domain basis function method. *IEEE Trans. Antennas Propagat.*, 52(11), 3078-3085.

[33] Lucente, Eugenio, Monorchio, Agostino, & Mittra, Raj. (April 2008). An iteration-free MoM approach based on excitation independent characteristic basis functions for solving large multiscale electromagnetic scattering problems. *IEEE Antennas Propagat.*, 56(4), 999-1007.

[34] Maaskant, R., Mittra, R., & Tijhuis, A. (November 2008). Fast analysis of large antenna arrays using the characteristic basis function method and the adaptive cross approximation algorithm. *IEEE Trans. Antennas Propagat.*, 56(11), 3440-3451.

[35] Matekovits, L., Laza, V. A., & Vechhi, G. (September 2007). Analysis of large complex structures with the synthetic-functions approach. *IEEE Trans. Antennas Propagat.*, 55(9), 2509-2521.

[36] MathWorks. (2009). Matlab Getting Started Guide. http://www.mathworks.com.

[37] Misra, P., & Naishadham, K. (December 1996). Order-recursive gaussian elimination (ORGE) and efficient CAD of microwave circuits. *IEEE Trans. Microwave Theory Tech.*, 44(12), 2166-2173.

[38] Ooms, S., & DeZutter, D. (March 1998). A new iterative diakoptics-based multilevel moments method for planar circuits. *IEEE Trans. Microw. Theory Tech.*, MTT-46(3), 280-291.

[39] Prakash, V.V.S., & Mittra, R. (January 2003). Characteristic basis function method: A new technique for efficient solution of method of moments matrix equation. *Microwave Opt. Technol. Lett.*, 36(2), 95-100.

[40] Rao, S. M., Wilton, D. R., & Glisson, A. W. (May 1982). Electromagnetic scattering by surfaces of arbitrary shape. *IEEE Trans. Antennas Propagat.*, AP-30, 409-418.

[41] Rousseau, P. R., & Burkholder, R. J. (October 1995). A hybrid approach for calculating the scattering from obstacles within large, open cavities. *IEEE Trans. Antennas Propagat.*, 43(10), 1068-1075.

[42] Song, J. M., Lu, C. C., & Chew, W. C. (October 1997). Multilevel fast multipole algorithm for electromagnetic scattering by large complex objects. *IEEE Trans. Antennas Propagat.*, 45(10), 1488-1493.

[43] Suter, Eric, & Mosig, Juan R. (August 2000). A subdomain multilevel approach for the efficient MoM analysis of large planar antennas. *Microwave Opt. Technol. Lett.*, 26(4), 270-277.

[44] Vegni, L., Toscano, A., & Popovski, B. (1997). Electromagnetic plane wave scattering by large and finite strip array on dielectric slab. *Ann. Telecommun.*, 52(3-4), 209-218.

[45] Waller, M. L., & Rao, S. M. (October 2002). Application of adaptive basis functions for a diagonal moment matrix solution of arbitrarily shaped three-dimensional conducting body problems. *IEEE Trans. Antennas Propagat.*, 50(10), 1445-1452.